TRANSACTIONS ON ELECTRICAL AND ELECTRONIC MATERIALS
Vol. 18, No. 2, pp. 93-96, April 25, 2017

Regular Paper

pISSN: 1229-7607 eISSN: 2092-7592
DOI: https://doi.org/10.4313/TEEM.2017.18.2.93
OAK Central: http://central.oak.go.kr

Characteristics of Ti Thin films and Application as a Working Electrode in TCO-Less Dye-Sensitized Solar Cells

Yong Hwan Joo and Nam-Hoon Kim
Department of Electrical Engineering, Chosun University, Gwangju 61452, Korea

Yong Seob Park†
Department of Electronics, Chosun College of Science and Technology, Gwangju 61453, Korea

Received December 16 2016, Revised April 3, 2017, Accepted April 4, 2017

The structural, electrical and optical properties of Ti thin films fabricated by dual magnetron sputtering were investigated under various film thicknesses. The fabricated Ti thin films exhibited uniform surfaces, crystallinity, various grain sizes, and with various film thicknesses. Also, the crystallinity and grain size of the Ti thin films increased with the increase of film thickness. The electrical properties of Ti thin films improved with the increase of film thickness. The results showed that the performance of TCO-less DSSC critically depended on the film thickness of the Ti working electrodes, due to the conductivity of Ti thin film. However, the maximum conversion efficiency of TCO-less DSSC was exhibited at the condition of 100 nm thickness due to the surface scattering of photons caused by the variation of grain size.

Keywords: Ti thin film, Magnetron sputtering, Dye-sensitized solar cell, Resistivity

1. INTRODUCTION

Dye-sensitized solar cells (DSSCs), a new generation of photovoltaic technology, have been intensively investigated in the solar cell industry and academia as a feasible candidate to replace conventional silicon-based photovoltaic cells because of their simple fabrication, low manufacturing cost, and high power conversion efficiency (PCE) compared to silicon-based and thin-film photovoltaic cells [1,2]. Typical DSSCs are composed of a working electrode (WE) with transparent conductive oxides (TCOs), mesoporous anatase titanium dioxide (TiO_2) nanocrystals with ruthenium-based dyes, an electrolyte of a redox couple (I_3^-/I^-), and a counter electrode (CE) [3]. Fluorine-doped tin oxide (FTO-glass) in TCOs is typically used as the WE because of its outstanding catalytic activity toward reducing I_3^-, excellent thermal stability, relatively low surface resistance, and high transmissivity of over 80% [2,4]. However, the cost of FTO-glass is estimated to be over 40% of the module cost [5], which prevents the commercialization of DSSCs. Alternative materials and structures need to be developed in order to reduce the module costs for use in DSSCs. The above-mentioned disadvantage can be resolved using TCO-less DSSCs by replacing the TCO layer with a metal layer at the rear side of TiO_2/dye layer.

In this study, a sputtered titanium (Ti) metal layer was applied for the WE of the back contact in TCO-less DSSCs. Ti, which is a light and abundant metal, has good mechanical properties, remarkably high corrosion resistance, low thermal expansion, and low resistivity [6,7]. The structural, electrical, and optical properties of Ti thin films, deposited by dual magnetron sputtering with a variation of thicknesses, were examined. TCO-less DSSCs, with Ti thin films as the WE, were fabricated and their photovoltaic performance was then analyzed.

2. EXPERIMENTS

Ti thin films were deposited on glass and *p*-type (100) silicon (Si) substrates by a specially designed dual magnetron sputtering system at room temperature. Two targets of pure (99.99%) 4-inch Ti,

† Author to whom all correspondence should be addressed:
E-mail: yongspark@cst.ac.kr

each with a diameter of 10.16 cm, were positioned about 6 cm from the substrate. The substrates were cleaned in trichloroethylene, acetone, methanol, and deionized water for 10 min in each solution and were then etched in hydrofluoric acid to strip the native oxide before deposition. After successive cleaning, the samples were dried in flowing nitrogen gas. After loading of the substrates, the base pressure and working pressure of the Ti targets were maintained at 2×10^{-3} Torr. Argon (99.99%) was used as the sputtering gas and the rotation speed of substrate for all depositions was kept constant at 15 rpm for uniform deposition. The DC power of the Ti targets was fixed at 50 W. Under these conditions, the thickness of the Ti thin films was set at 50, 100, 200, and 300 nm in different samples by controlling the sputtering time. The structural, electrical, optical, and morphological properties of the sputtered Ti thin films were examined, and the TCO-less DSSCs were then fabricated using the Ti thin films. To fabricate the TCO-less DSSCs, an adhesion layer of 10 nm-thick Ti thin films was deposited on the pure glass substrates without FTO coating. The sputtered Ti thin films were then coated with nanocrystalline titanium dioxide (TiO_2) photoanode of 10 μm-thickness. The nanocrystalline TiO_2 was sintered in a furnace at 550℃ for 60 minutes, and the Ti thin films with the various thicknesses were then deposited on the nanocrystalline TiO_2 to fabricate the WE. Dye (N719) was adsorbed into TiO_2 by immersing the TiO_2 in the dye for 24 hours following the deposition of Ti thin films. The CE was prepared by sintering at 450℃ for 30 minutes after coating $PtCl_4$ on the FTO-glass with two holes. WE and CE were sealed with sealant, and electrolyte was then injected into the holes.

The surface morphology and thickness of all thin films were measured by using atomic force microscopy (AFM, NITECH, SPM 400, operated in contact mode with a Si-DF40 tip) and field emission scanning electron microscopy (FESEM, Philips, XL-40aFEG, 10 kV). The crystalline structures were characterized using an X-ray diffractometer (XRD: Bruker, AXS D8 Discover, Cu Kα = 0.15405 nm, 40 kV, 30 mA) in the range of 20~80° 2θ with a measurement step of 0.02°. The transmittance and reflectivity of Ti films were measured using Cary 500 Scan measurement (Varian COMPANY). The electrical characteristics were measured using a 4-point probe (CHANG MIN Co. Ltd., CMT-ST1000). Photovoltaic performance was evaluated using a solar simulator (Abet Technologies, 30W Xe lamp, AM1.5).

3. RESULTS AND DISCUSSION

Figure 1 shows the FESEM cross-sectional image of Ti thin films of 50 nm and 300 nm thickness fabricated by the dual magnetron sputtering method. As the thickness of the thin films increased, small crystallites were observed in a vertical direction on the surface of the Ti thin films. This result is related to the surface temperature generated on the surface during the sputtering deposition of metal ions, which affects the crystallinity of thin films and contributes to the density and orientation of crystals. In other words, the increase in the deposition time of thin films increases the temperature due to the sputtering effect of increased ions on the surface of thin films; the increased temperature then contributes to the increase of the density and crystallinity of thin films, which finally influences the increase in grain size the grain size [8].

Figure 2 shows the surface images of Ti thin films with thicknesses of 50 nm and 300 nm analyzed using the AFM. As seen from the surface, the surface morphologies show uniform and smooth surfaces regardless of film thickness. As shown by the measured values of the root mean square (RMS) surface roughness (R_{ms}) according to the thickness, the R_{ms} surface roughness value of Ti thin films increased from 3.2 nm to 7.4 nm as the thickness of Ti thin films was increased. As confirmed by FESEM results, this the increase in R_{ms} is related to the increased surface temperature

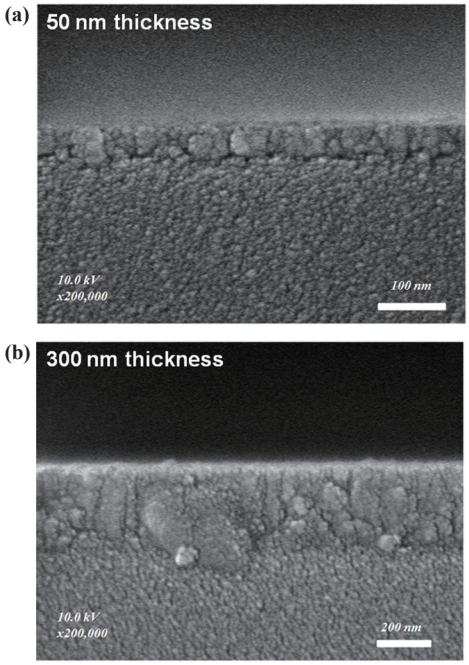

Fig. 1. FESEM cross-sectional images of Ti film of (a) 50 nm and (b) 300 nm thick fabricated by sputtering method.

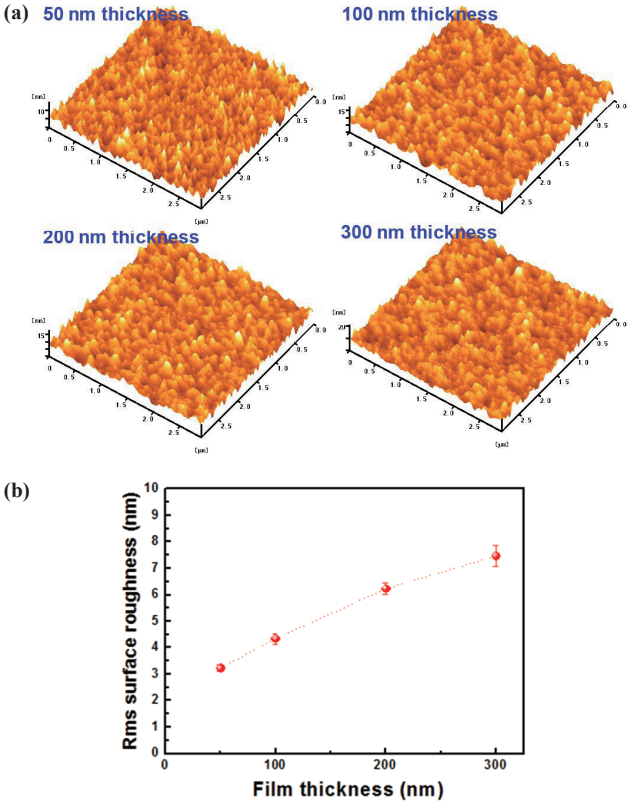

Fig. 2. (a) AFM surface images of Ti thin films with various thickness from 50 nm to 300 nm and (b) R_{ms} surface roughness of Ti thin films fabricated with the increase of film thickness.

during sputtering, and the increase of the surface temperature of thin films contributed to the crystallinity of thin films. In other words, the increase in deposition time enhanced the sputtering effect on the surface of thin films, and the increase of density and

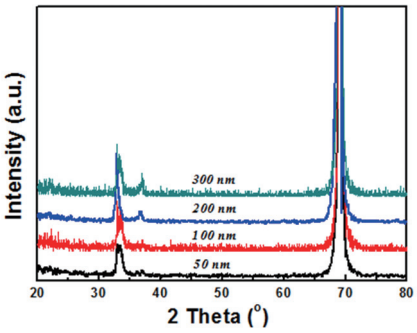

Fig. 3. XRD patterns of Ti films fabricated with various film thicknesses.

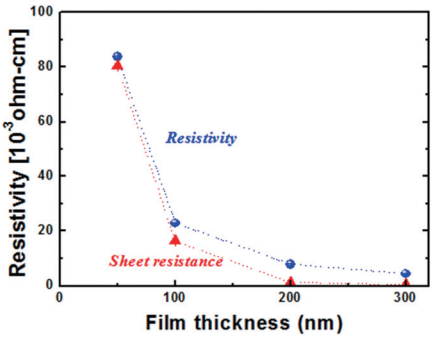

Fig. 4. Resistivity and sheet resistance of Ti films fabricated with various film thicknesses.

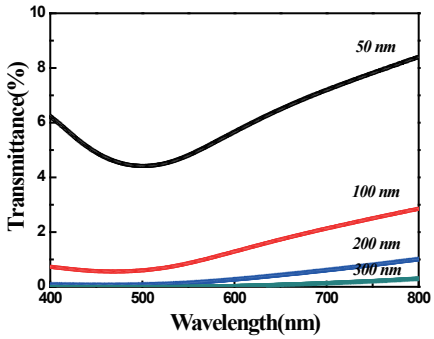

Fig. 5. Transmittance of Ti films fabricated with various film thicknesses.

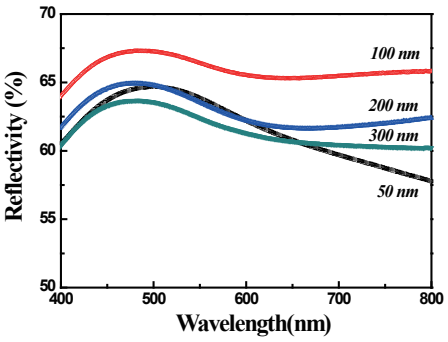

Fig. 6. Reflectivity of Ti films fabricated with various film thicknesses.

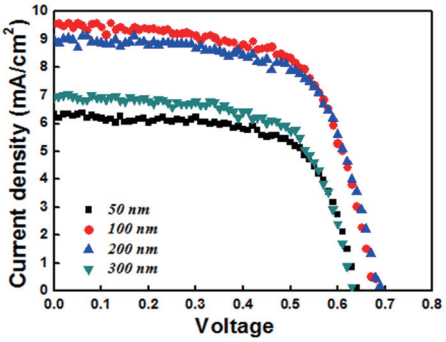

Fig. 7. Current density-voltage curves of TCO-less DSSCs using Ti working electrodes prepared with various film thicknesses.

crystallinity of the thin films resulting from the increased surface temperature was due to the increased grain size of the surface, which led to the increase in surface roughness [8,9].

Figure 3 shows the XRD pattern of Ti thin films with various thicknesses fabricated by a sputtering method. As seen in the XRD pattern, the peak intensity of the Ti (100) orientation was slightly increased with the increased thickness of the Ti thin films. Also, the crystal size was determined by the Gaussian fitting method from the XRD diffraction pattern. The maximum half width of the angle and diffraction peak was obtained by Gaussian fitting. By substituting into the following formula used to obtain the crystal size, the crystal size increased as the deposition time increased or as the film thickness increased. These results can be explained by the increase of the sputtered ions on the surface, which is attributed to the increase of the surface temperature on the substrate. These results confirmed that, as the thickness of thin films increased, the crystallinity also increased; the grain size of the surface of thin films consequently increased [9,10]. The change of the grain size of the surface of thin films is considered to affect the improvement of electrical conductivity.

$L=(0.89\times\lambda)/\beta\cos\theta$

$\lambda = 0.154$

β = Maximum half width of the diffraction peak

Figure 4 shows the changes in the values of resistivity and surface resistance of the fabricated Ti thin films according to the thickness of thin films. The resistivity and surface resistivity decreased as the thickness of Ti thin films increased. The minimum values of resistivity and surface resistance were found to be 4.5 m$\Omega\cdot$cm and 0.23 Ω/square, respectively, when the thickness of the Ti thin film was 300 nm. As the thickness of the thin films was increased, their crystallinity increased, which contributed to the reduction of the resistivity and surface resistance of the thin films [11-13].

Figures 5 and 6 show the transmittance and reflectivity of Ti films fabricated with various film thicknesses, respectively. As shown in the figures, the transmittance of Ti thin films decreased with the increase of film thickness and the highest reflectivity of the films is exhibited at the condition of 100 nm thickness. In the DSSC structure, DSSC efficiency is related to the TiO_2 light absorption layer, and the efficiency depends on the amount of light absorbed in the TiO_2 light absorption layer of the DSSC structure. From the results, the reflectance of Ti thin film shows the largest value at the thickness of 100 nm. Consequently, the Ti electrode thickness of 100 nm is considered to be the optimal condition for light absorbtion by the TiO_2 light absorption layer.

Figure 7 shows the electrical properties of the TCO-less DSSC with a Ti working electrode depending on the thickness of the Ti film. For the cell characteristics of solar cells, current-voltage characteristics were examined by irradiating light under the condition of AM-1.5 (300W xenon lamp, 100 mW/cm^2), and the characteristics of the solar cells were confirmed from the values of the open-circuit voltage (V_{oc}), short-circuit current density

Table 1. Photovoltaic performance data of TCO-less DSSCs using Ti working electrodes prepared with various film thicknesses.

Condition	V_{oc} (mV)	J_{sc} (mA/cm^2)	FF	CE (%)
50 nm	640	6.34	0.66	2.67
100 nm	680	9.56	0.65	4.21
200 nm	690	8.99	0.65	4.04
300 nm	630	6.94	0.67	2.94

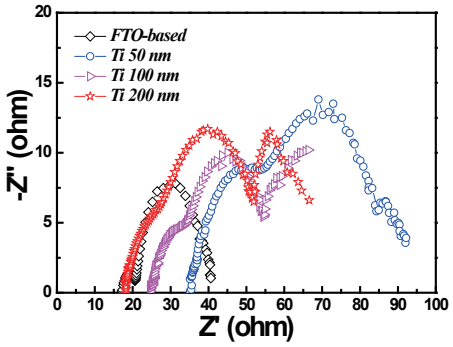

Fig. 8. Nyquistplot of TCO-less DSSCs by using various Ti working electrode thicknesses.

(J_{sc}), fill factor (FF), and conversion efficiency (CE). Figure 7 and Table 1 show that the maximum CE of the TCO-less DSSC was observed when a Ti working electrode with a thickness of 100 nm was applied to the TCO-less DSSC. In this case, the values of CE, J_{sc}, V_{oc}, and FF were found to be 4.21%, 9.56 mA/cm^2, 680 mV, and 0.65, respectively. It was confirmed that the changes in J_{sc} and FF were closely related to the changes in the resistance of thin films depending on the variation of the thickness of the Ti thin films, and that the changes in the thickness of thin films were due to the changes in equivalent series resistance. However, the conversion efficiency of TCO-less DSSC was found to decrease when the thickness of the Ti thin film was 200 nm or more. These results showed that as the thickness of metallic thin films increased, the crystallinity of the thin films increased, and the grain size of the surface also increased. Such changes in the grain size of the surface resulted in a greater loss of the light that was incident on and transmitted through the TiO_2 photoanode from the thin film surface of the electrode. The changes in the grain size of the surface also decreased the electron generation rate due to the reduction of the adsorption rate between the photoanode and the dye due to light scattering, which is believed to have affected a reduction of J_{sc} and an increase in the equivalent series resistance of the electrode [14,15].

Figure 8 shows the EIS spectra obtained for various Ti film thicknesses. The 3 semicircular shapes at the EIS spectra for DSSC are related to the charge transport at the Pt counter electrode (R_1; high-frequency region), at the TiO_2/dye/Ti layer/electrolyte interface (R_2; middle-frequency region), and in Nernstian diffusion within the electrolyte (RD; low-frequency region), respectively [16,17]. From the figure, the total series impedance is decreased with the increase of film thickness. These results are explained by the reduction of sheet resistance with the increase of Ti thickness. And also, it is reported that the fill factor is decreased by the increase of total series resistance [16,17]. However, in this work, the fill factor is similar with various film thicknesses.

4. CONCLUSIONS

In this study, a Ti metal electrode was suggested as the electrode material for fabricating DSSCs without the TCO. Thin films were fabricated by a sputtering device. It was observed that, as the thickness of the Ti metal electrodes was increased, the values of resistivity and surface resistance decreased, the electrical conductivity improved, and the surface roughness increased. Consequently, the increase in the thickness of thin films led to their increased crystallinity, which resulted in the increase in the grain size of the surface of the thin films. These changes reduced the transmission of light, resulting in a loss of light due to the light scattering. In conclusion, the maximum value of the conversion efficiency of TCO-less DSSCs with Ti WE was observed when the thickness of the Ti thin film was 100 nm. It is suggested in this study that this is due to the optimization of the conduction characteristics, transmission properties, and surface properties of the Ti thin films.

REFERENCES

[1] S. Yun, P. D. Lund, and A. Hinsch, *Energy Environ. Sci.*, **8**, 3495 (2015). [DOI: https://doi.org/10.1039/C5EE02446C]

[2] G. Kang, J. Choi, and T. Park, *Sci. Rep.*, **6**, 22987 (2016). [DOI: https://doi.org/10.1038/srep22987]

[3] S. Suhaimi , M. M. Shahimin, Z. A. Alahmed, J. Chyský, and A. H. Reshak, *Int. J. Electrochem. Sci.*, **10**, 2859 (2015).

[4] Z. Chen, W. Li, R. Li, Y. Zhang, G. Xu, and H. Cheng, *Langmuir*, **29**, 13836 (2013). [DOI: https://doi.org/10.1021/la4033282]

[5] H.-G. Yun, M. Kim, M. G. Kang, and I.-H. Lee, *Phys. Chem. Chem. Phys.*, **14**, 6448 (2012). [DOI: https://doi.org/10.1039/c2cp40205j]

[6] N. Muslim, Y. W. Soon, C. M. Lim, and N. Y. Voo, *ARPN J. Eng. Appl.Sci.*, **10**, 7184 (2015).

[7] K. Buijs, *Stainless Steel World*, **17**, 1 (2005).

[8] Y. M. Lu, W. S. Hwang, W. Y. Liu, and J. S. Yang , *Mater. Chem. Phys.*, **72**, 269. (2001). [DOI: https://doi.org/10.1016/S0254-0584(01)00450-3]

[9] Y. L. Jeyachandran, B. Karunagaran, S. K. Narayandass, and D. Mangalaraj, *Mat. Sci. Eng. A-Struct.*, **458**, 361 (2007). [DOI: https://doi.org/10.1016/j.msea.2006.12.088]

[10] K. Hofmann, B. Spangenberg, M. Luysberg, and H. Kurz, *Thin Solid Films*, **436**, 168 (2003). [DOI: https://doi.org/10.1016/S0040-6090(03)00582-0]

[11] S. Schiller, G. Beister, W. Sieber, G. Schirmer, and E. Hacker, *Thin Solid Films*, **83**, 239 (1981). [DOI: https://doi.org/10.1016/0040-6090(81)90673-8]

[12] A. Grill, *Surf. Coat. Technol.*, **94**, 507 (1997). [DOI: https://doi.org/10.1016/S0257-8972(97)00458-1]

[13] A. Czyzniewski, *Thin Solid Films*, **433**, 180 (2003). [DOI: https://doi.org/10.1016/S0040-6090(03)00324-9]

[14] L. J. Meng and M. P. dos Santos, *Thin Solid Films*, **226**, 22 (1993). [DOI: https://doi.org/10.1016/0040-6090(93)90200-9]

[15] L. Han, N. Koide, Y. Chiba, A. Islam, R. Komiya, N. Fuke, A. Fukui, and R. Yamanaka, *Appl. Phys. Lett.*, **86**, 213501 (2005). [DOI: https://doi.org/10.1063/1.1925773]

[16] L. Han, N. Koide, Y. Chiba, and T. Mitate, *Appl. Phys. Lett.*, **84**, 2433 (2004).

[17] M. Adachi, M. Sakamoto, J. Jiu, Y. Ogata, and S. Isoda, J. *Phys. Chem.* **B**, **110**, 13872 (2006).